Am J Transl Res 2022;14(11):8129-8145
www.ajtr.org /ISSN:1943-8141/AJTR0146620

Original Article

MiR-216b targets CPEB4 to suppress colorectal cancer progression through inhibiting IL-10-mediated M2 polarization of tumor-associated macrophages

Jun Zou[1], Boyu Wu[2], Chao Lin[1], Qunhua Ding[1], Jiangtao Li[3]

[1]Department of Abdominal Surgery, Jiangxi Cancer Hospital, Nanchang 330029, Jiangxi, China; [2]Department of General Surgery, Shangrao Municipal Hospital, Shangrao 334000, Jiangxi, China; [3]Department of Hepato-Biliary-Pancreatic Surgery, The First Affiliated Hospital, Hengyang Medical School, University of South China, Hengyang 421001, Hunan, China

Received September 20, 2022; Accepted October 18, 2022; Epub November 15, 2022; Published November 30, 2022

Abstract: Objectives: The M2 polarization of tumor-associated macrophages (TAMs) facilitates the growth, invasion and metastasis of tumor cells. Here, we investigated the role of miR-216b in the M2 polarization of TAMs in colorectal cancer (CRC). Methods: The expression of genes were examined by quantitative real-time polymerase chain reaction, Western blot, enzyme-linked immunosorbent assay and immunohistochemistry. The relationship between miR-216b and CPEB4 was verified through dual luciferase reporter assays. The proliferation, migration and invasiveness of CRC and Raw264.7 cells were assessed through cell counting kit-8 and Transwell assays. Flow cytometry was used to quantify the percentage of F4/80+/CD206+RAW264.7 cells. The metastasis of tumor cells in liver and lung tissues was evaluated by establishing a mouse xenograft tumor model and hematoxylin-eosin staining. Results: Downregulation of miR-216b enhanced the M2 polarization of TAMs. CPEB4 was identified as a target of miR-216b. CPEB4 knockdown suppressed CRC cell proliferation, migration and invasion, which were rescued by miR-216b inhibition. It was confirmed that M2 macrophage infiltration in CRC was positively correlated with the expression levels of CPEB4 and IL-10. CPEB4 knockdown impaired the M2 polarization of Raw264.7 cells and reduced IL-10 expression. miR-216b overexpression suppressed tumor growth, metastasis and expressions of CPEB4, CD206 and IL-10 in CRC xenograft models. Conclusions: miR-216b targets CPEB4 to impair the IL-10-mediated M2 polarization of TAMs, thereby inhibiting CRC development.

Keywords: Colorectal cancer, miR-216b, CPEB4, IL-10, tumor-associated macrophages, M2 polarization

Introduction

Colorectal cancer (CRC) is a common malignancy, with over 1.4 million new cases annually [1, 2]. Approximately 41% of CRCs occur in the proximal colon, 28% in the rectum and 22% in the distal colon [3]. CRC causes 694,000 deaths annually and is a major global healthcare issue [4]. Despite advances in surgical resection, radiotherapy and chemotherapy, metastasis and therapeutic failure are still common [5-7]. New and more effective anti-CRC therapies are therefore urgently required.

The tumor microenvironment (TME) is composed of cancer cells, cancer-related fibroblasts, immune cells and non-cellular components [8], and dictates tumor occurrence, growth and metastasis [9, 10]. As the most abundant immune cells in the TME, tumor-associated macrophages (TAMs) produce cytokines and chemokines to suppress anti-tumor responses, enhancing the proliferation, metastasis and invasiveness of tumor cells [11, 12]. M2 TAMs, which are generated through M2 polarization, induce the epithelial-mesenchymal transformation of tumor cells to promote CRC metastasis [13, 14]. Moreover, M2 TAMs produce anti-inflammatory cytokines, including IL-10, IL-13 and TGF-β, to promote tumor development [15]. To date, the carcinogenicity of M2 TAMs has been widely explored, but the mechanisms governing the M2 polarization of TAMs remains poorly understood.

Table 1. Primer sequences for cell transfection

Gene	Sequence (5'-3')
miR-216b mimic	AAAUCUCUGCAGGCAAAUGUGA
	ACAUUUGCCUCCAGAGAUUUUU
mimic-negative control	UUCUCCGAACGUGUCACGUTT
	ACGUGACACGUUCGGAGAATT
miR-216b inhibitor	AAAUCUCUGCAGGCAAAUGUGA
inhibitor NC	CAGUACUUUUGUGUAGUACAA
sh-CPEB4	CCACAGCTTCTTACTAAGTTT
Sh-NC	TTTTCCGAACGTGTCACGTTT

MicroRNAs (miRNAs) are short non-coding RNAs (19-25 nucleotides in size) that modulate the post-transcriptional silencing of target genes [16-18]. MiR-145, miR-934 and miR-106b modulate the M2 polarization of TAMs in CRC [19-21]. MiR-203 and miR-1246 have been shown to influence CRC development [22]. MiR-216b exerts anti-tumor effects in CRC [23-25], but its effects on TAMs have not been elucidated.

Cytoplasmic polyadenylation element-binding protein 4 (CPEB4) [26] has been shown to enhance the M2 polarization of macrophages in CRC [27-29]. CPEB4 is targeted by several miRNAs, including miR-758-3p, miR-145-5p and miR-874-3p [30-32]. Bioinformatics analysis has shown that CPEB4 positively correlates with the M2 polarization of macrophages and IL-10 expression in CRC cells. However, the regulatory mechanisms governed by miR-216b and CPEB4 have not been explored at the molecular level in CRC.

Here, we investigated the role of miR-216b and CPEB4 in macrophage polarization and CRC progression.

Materials and methods

Cell culture

CRC cell lines (MC38 and HCT116) and murine macrophages (RAW264.7) were purchased from the cell bank of the Chinese Academy (Shanghai, China). Cells were maintained in Dulbecco's Modified Eagle Medium (DMEM, Thermo Fisher Scientific, Waltham, MA, USA) supplemented with 10% fetal bovine serum (FBS, Sigma, St. Louis, MO, USA) and 1% penicillin/streptomycin (Sigma). Cells were grown in a 5% CO_2 incubator at 37°C. For co-culture experiments, MC38 cells or HCT116 cells were co-cultured with RAW264.7 cells for 24 h.

MiRNA transfections

MiR-216b mimic, mimic-negative control (NC), miR-216b inhibitor and inhibitor NC were purchased from Genepharma (Shanghai, China). Short hairpin RNAs targeting CPEB4 (sh-CPEB4), sh-NC, pcDNA3.1-CPEB4 (full length) and pcDNA3.1-NC (its tag in-frame with the 3'-end, CMV promoter, neomycin resistant gene) were purchased from Ribio (Beijing, China). Plasmids were transfected using Lipofectamine 3000 (Invitrogen). The primer sequences are shown in **Table 1**.

CRC conditioned media

MC38 or HCT116 cells were cultured in DMEM containing 10% FBS for 72 h. Upon reaching 80%-90% confluency, cells were treated with serum free media for 24 h, centrifuged at 2,000 g and filtered (0.22-mm; Millipore, Billerica, MA, USA) to remove cell debris.

Quantitative real-time polymerase chain reaction (qRT-PCR) analysis

Total RNA was extracted through Trizol lysis (Invitrogen, Carlsbad, California, USA). RNA (2 μg) was reverse transcribed into cDNA using Primescript™ RT reagents (Vazyme, Nanjing, China). qRT-PCRs were performed using SYBR-Green PCR Master Mix (Vazyme, Nanjing, China). Reaction conditions were as follows: 95°C for 10 min, 45 cycles of 95°C for 20 s, 60°C for 20 s and 72°C for 30 s, and 72°C for 3 min. Primers (**Table 2**) were synthesized by Sangon (Shanghai, China). The relative mRNA expressions of Arg-1, Fizz-1, Ym-1, CD206, miR-216b, CPEB4 and IL-10 were normalized to GAPDH or U6 using the $2^{-\Delta\Delta Ct}$ method.

Dual luciferase reporter assays

Wild type (WT) and mutant (MUT) CPEB4 3'-UTR sequences containing putative miR-216b binding sites were cloned into pGL3-Basic (Promega, Shanghai, China). Plasmids were co-transfected with NC/miR-216b mimic into Raw264.7 cells using Lipofectamine 3000 (Invitrogen). Forty-eight hours post-transfection, Firefly and

Table 2. Primer sequences for qRT-PCR analysis

Gene		Sequences (5'-3')
Arg-1	Forward	TGTCCCTAATGACAGCTCCTT
	Reverse	GCATCCACCCAAATGACACAT
Fizz-1	Forward	CCAATCCAGCTAACTATCCCTCC
	Reverse	ACCCAGTAGCAGTCATCCCA
Ym-1	Forward	CAGGTCTGGCAATTCTTCTGAA
	Reverse	GTCTTGCTCATGTGTGTAAGTGA
CD206	Forward	CTCTGTTCAGCTATTGGACGC
	Reverse	TGGCACTCCCAAACATAATTTGA
MiR-216b	Forward	GCCGCGCTAAAGTGCTTA
	Reverse	CACCAGGGTCCGAGGT
IL-10	Forward	CTTACTGACTGGCATGAGGATCA
	Reverse	GCAGCTCTAGGAGCATGTGG
CPEB4	Forward	TGCTATCCATTCTCGTGCTG
	Reverse	AGCGTGAAGAGGTTGAGGAA
U6	Forward	TGCGGGTGCTCGCTTCGGC
	Reverse	CCAGTGCAGGGTCCGAGGT
GAPDH	Forward	AGGTCGGTGTGAACGGATTTG
	Reverse	GGGGTCGTTGATGGCAACA

Renilla activity were assessed through dual luciferase reporter assays.

Cell counting kit (CCK) assays

CCK-8 (Beyotime, Shanghai, China) assays were used to measure cell proliferation. Briefly, cells (1×10^3 cells/well) were seeded into 96-well plates for 0, 24, 48, 72 and 96 h and treated with CCK-8 reagent. Absorbances were read on a microplate reader (MG LABTECH, Durham, NC, USA) at 450 nm.

Flow cytometry

M2-like macrophage markers in RAW264.7 cells were detected by flow cytometry. Briefly, cells in 6-well plates were fixed, blocked in 3% bovine serum albumin and probed with PE-conjugated anti-mouse CD206 (1:100, eBiosciences, San Diego, CA, USA) and FITC-conjugated anti-mouse F4/80 (1:200, eBioscience) for 1 h. Cells were assessed on a FACSCalibur (Becton Dickinson, San Jose, CA, USA).

Transwell assays

Cells were seeded into the upper chambers of Transwell Boyden Chambers (8-μm pore size; Costar, Bethesda, MD, USA) coated with BD Matrigel™ Matrix Basement Membrane (Becton Dickinson) in serum-free medium. Medium (600 μL) plus 10% FBS were added to the lower chambers. Cells were incubated for 24 h, fixed in paraformaldehyde and labeled with crystal violet. Invading cells were imaged on a light microscope.

Western blotting

Cells were lysed in RIPA buffer (Beyotime), and protein concentrations were measured via BCA assay (Thermo Fisher Scientific). Proteins were resolved by SDS gel electrophoresis and transferred to polyvinylidene difluoride membranes. Membranes were blocked in skimmed milk and probed with primary antibodies against CPEB4 (1:1000, #28748, Cell Signaling Technology, Danvers, Massachusetts, USA), Arg-1 (1:1000, #93668, Cell Signaling Technology), Fizz-1 (1:1000, ab39626, Abcam, Cambridge, MA, USA), Ym-1 (1:10000, ab192029, Abcam), CD206 (1:1000, ab17942, Abcam), IL-10 (1:1000, ab133575, Abcam) and β-actin (1:200, ab115777, Abcam) overnight at 4°C. Membranes were then washed and labeled with HRP-conjugated secondary antibodies (1:2000, ab6721, Abcam) for 1 h. Proteins were visualized on a Bioimaging system (Bio-Rad, Berkeley, California, USA), and quantified using Image J software (NIH, Bethesda, MD, USA).

Enzyme-linked immunosorbent assay (ELISA)

Cell supernatants were collected, and the levels of IL-10 were assayed using commercial ELISA Ready-Set-Go kits (eBioscience). Blocking solution was included as a positive control.

Animal models

BALB/c nude mice (6-7 weeks, female) were purchased from the Experimental Animal Center of Southern Medical University (Guangzhou, China). Animal experiments were performed in compliance with guidelines of the Institutional Animal Care and Use Committee of Jiangxi Cancer Hospital NIH's Guide for the Care and Use of Laboratory Animals. The study protocol was approved by the Animal Medical Ethics Committee of Jiangxi Cancer Hospital (2022ky096). To explore the role of miR-216b in CRC *in vivo*, HCT116 cells (5×10^5 cells in 0.2 mL PBS) stably transfected with miR-216b

mimic or mimic NC were subcutaneously injected into the right flank of mice [33]. Mice were divided into 2 groups (n = 6/group). Tumor sizes were monitored once a week, and tumor volumes were calculated using the formula V = (shortest diameter)^2 × (longest diameter) × 0.5. After 5 weeks, blood was obtained from tails for ELISA analysis, and mice were sacrificed via cervical dislocation. Tumors were collected for weight measurements and immunohistochemistry (IHC) staining. Lung tissues and liver tissues were collected for hematoxylin-eosin (H&E) staining.

IHC staining

Tumor tissues were fixed in formalin and embedded in paraffin. Tissues were then cut into 4 μm sections, dewaxed and rehydrated. Following antigen repair and blocking, sections were probed with antibodies against CPEB4 (1:200, ab16667, Abcam), CD206 (1:200, ab16667, Abcam) and IL-10 (1:200, ab16667, Abcam) at 4°C overnight. Sections were then labeled with anti-rabbit secondary antibodies (1:500, ab6112, Abcam) for 30 min and stained with 3,3'-diaminobenzidine substrate solution. Samples were counterstained with hematoxylin for 1 min and imaged under a microscope.

H&E staining

The right lungs of mice were fixed in paraformaldehyde, embedded in paraffin and cut into 5 μm sections. Sections were then deparaffinized and dehydrated. Thereafter, sections were stained using H&E staining kits (Beyotime) and imaged on an optical microscope.

Statistical analysis

Data are presented as mean ± standard deviation. Statistical analysis was performed using GraphPad Prism 7.0. Comparisons between two independent groups of data were performed using a Student's t test. Multigroup comparisons were performed using a one-way Analysis of Variance, accompanied by Tukey's test. $P < 0.05$ was regarded as statistically significant.

Results

MC38-derived conditioned medium (MC38 CM) promotes M2 polarization of Raw264.7 cells

We first sought to investigate the influence of MC38 CM on the M2 polarization of macrophages. Following MC38 CM treatment in Raw264.7 cells, increases were observed in the expressions of the M2 markers Arg-1, Fizz-1 and Ym-1 at both the mRNA and protein levels ($P < 0.01$, **Figure 1A**, **1B**). The expression of CD206 also increased in response to MC38 CM treatment ($P < 0.01$, **Figure 1C**, **1D**). Moreover, MC38 CM treatment significantly downregulated the expression of miR-216b ($P < 0.01$, **Figure 1E**).

We next investigated the influence of miR-216b on M2 polarization through its exogenous expression in Raw264.7 cells prior to CM treatment. miR-216b overexpression decreased the expressions of Arg-1, Fizz-1, Ym-1 and CD206 in response to MC38 CM-treatment ($P < 0.05$, **Figure 1F**, **1G**), the levels of which decreased following the downregulation of miR-216b ($P < 0.01$, **Figure 1H**, **1I**).

MiR-216b directly binds to CPEB4 and decreases CPEB4 expression

To probe the downstream mechanisms of miR-216b in Raw264.7 cells, the Targetscan database was used to predict targets of miR-216b. As shown in **Figure 2A**, the 3'-UTR of CPEB4 contained putative binding sites for miR-216b. Transfection of miR-216b mimic markedly decreased the relative luciferase activity of a CPEB4 WT reporter but not the relative luciferase activity of a CPEB4 MUT reporter in Raw264.7 cells ($P < 0.001$, **Figure 2B**). Expression of the miR-216b inhibitor increased CPEB4-WT reporter activity. miR-216b also decreased CPEB4 expression at both mRNA and protein levels. Transfection of a miR-216b inhibitor produced the opposite phenotype and markedly increased CPEB4 expression ($P < 0.01$, **Figure 2C**, **2D**).

MiR-216b suppresses the progression of CRC by targeting CPEB4

We then investigated whether miR-216b impacts CRC progression through targeting CPEB4. Transfection of the miR-216b mimic into MC38 and HCT116 decreased the expression of CPEB4, which increased following transfection of the miR-216b inhibitor ($P < 0.05$, **Figure 3A**, **3B**). In cells silenced for CPEB4, the proliferation of MC38 and HCT116 cells was markedly suppressed, whilst the overexpression of CPEB4 increased cell growth. Importantly, these effects of CPEB4 could be reversed by either miR-216b inhibition or over-

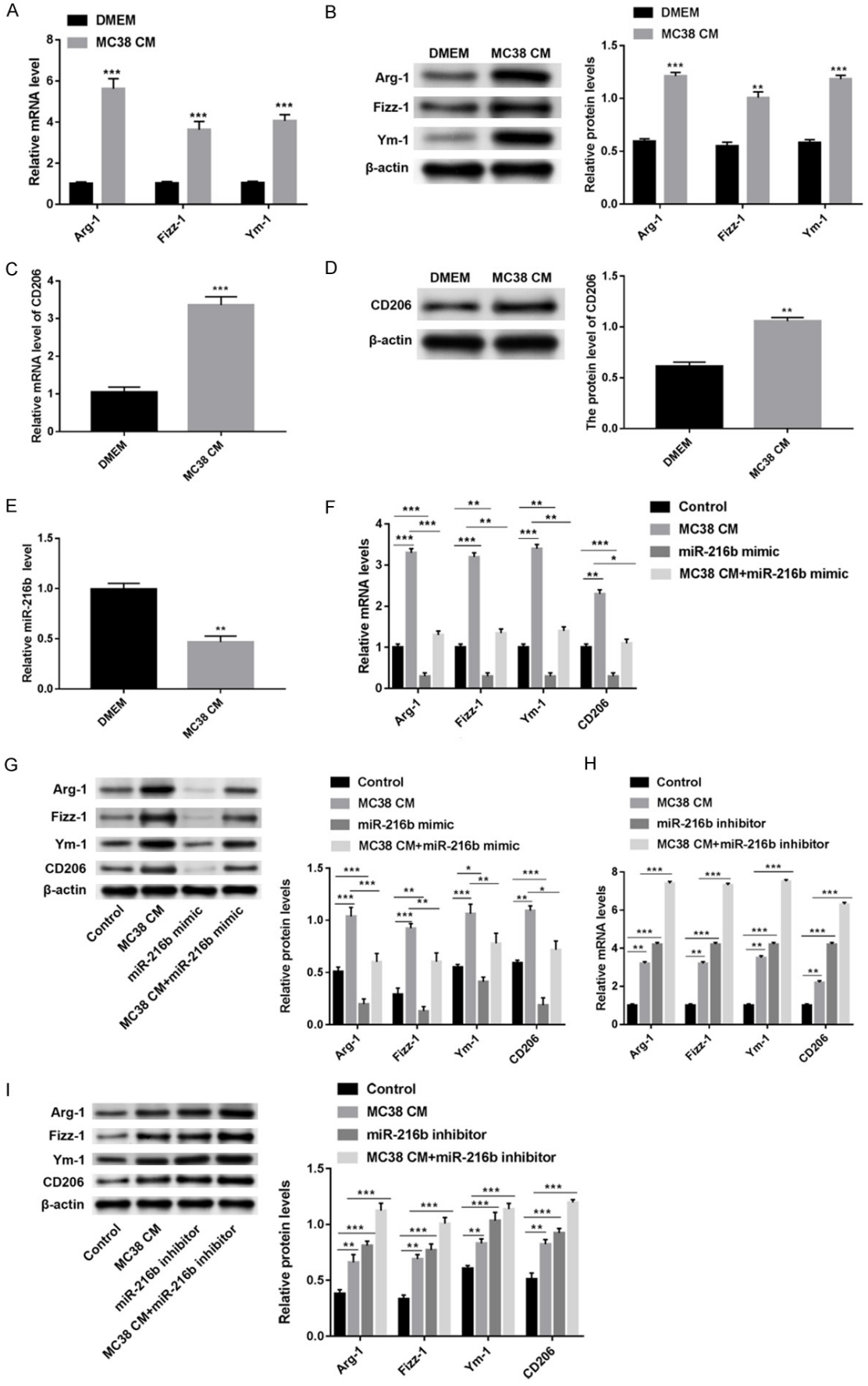
A
DMEM
MC38 CM
Relative mRNA level
Arg-1
Fizz-1
Ym-1
B
DMEM
MC38 CM
Arg-1
Fizz-1
Ym-1
β-actin
Relative protein levels
C
Relative mRNA level of CD206
D
CD206
β-actin
The protein level of CD206
E
Relative miR-216b level
F
Control
MC38 CM
miR-216b mimic
MC38 CM+miR-216b mimic
Relative mRNA levels
CD206
G
Relative protein levels
H
miR-216b inhibitor
MC38 CM+miR-216b inhibitor
I

Figure 1. MC38-derived conditioned medium promotes the M2 polarization of Raw264.7 cells. A. Relative mRNA expressions of Arg-1, Fizz-1 and Ym-1 detected by quantitative real-time polymerase chain reaction (qRT-PCR) in Raw264.7 cells. B. Relative expressions of Arg-1, Fizz-1 and Ym-1 assessed by Western blotting in Raw264.7 cells. C. Relative mRNA expression of CD206 assessed by qRT-PCR. D. Relative proteins expression of CD206 assessed by Western blotting. E. Relative mRNA expression of miR-216b examined by qRT-PCR in Raw264.7 cells. $^{*}P < 0.05$, $^{**}P < 0.01$, $^{***}P < 0.001$. F-I. Relative mRNA expressions of Arg-1, Fizz-1 and Ym-1 in Raw264.7 cells assessed by qRT-PCR and Western blotting. $^{*}P < 0.05$, $^{**}P < 0.01$, $^{***}P < 0.001$.

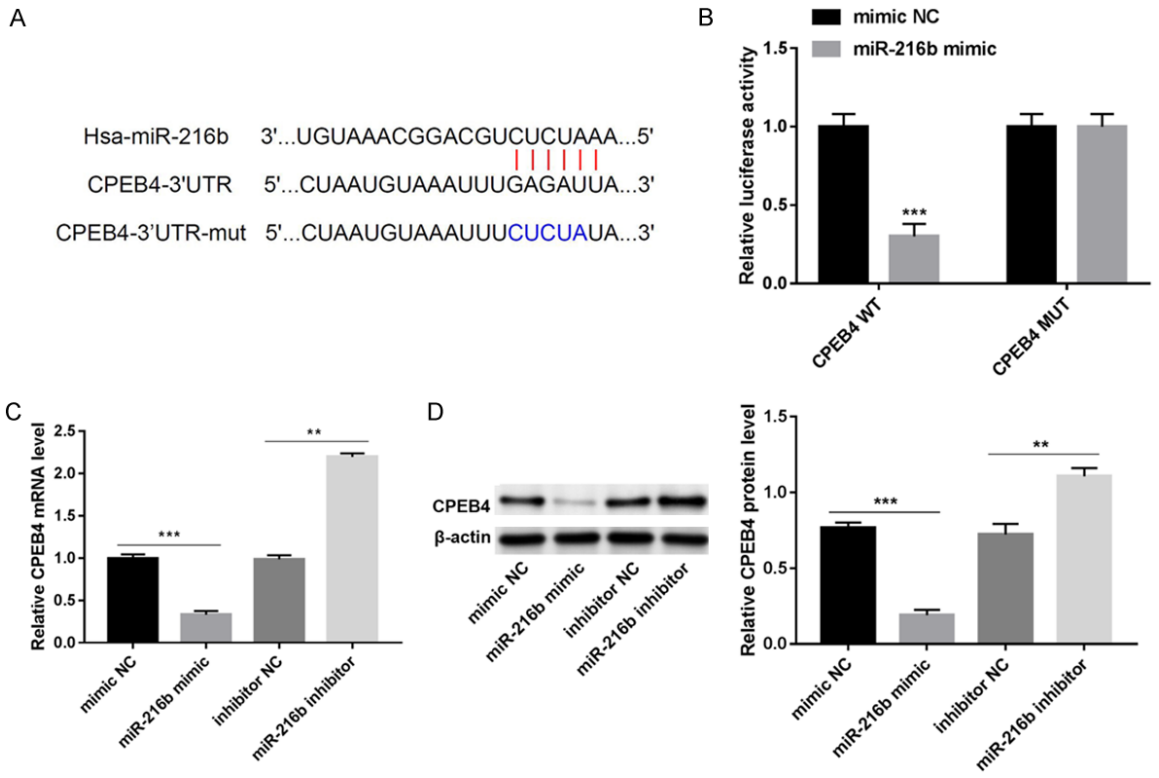

Figure 2. miR-216b directly binds to CPEB4 and decreases CPEB4 expression. A. Binding sequence of miR-216b and CPEB4 predicted by the Targetscan database. B. Interaction between miR-216b and CPEB4 in Raw264.7 cells by dual-luciferase reporter assays. C. Relative mRNA expression of CPEB4 in Raw264.7 cells detected by qRT-PCR. D. Relative expression of CPEB4 in Raw264.7 cells detected by Western blot. $^{**}P < 0.01$, $^{***}P < 0.001$.

expression ($P < 0.05$, **Figure 3C**, **3D**). Similarly, Transwell assays showed that CPEB4 knockdown reduced MC38 and HCT116 invasion, whilst CPEB4 overexpression increased the number of migrating and invading cells. These effects were again reversed by miR-216b inhibition or miR-216b overexpression, respectively ($P < 0.05$, **Figure 3E**, **3F**).

MiR-216b impairs IL-10 expression and M2 polarization of macrophages by regulating CPEB4 expression

M2 macrophages can be induced by several cytokines including IL-10, IL-4 and IL-13 [15]. Bioinformatics analysis showed that CPEB4 expression positively correlated with the infiltration of M2 macrophages and IL-10 expression in CRC (**Figure 4A**, **4B**). We therefore explored whether miR-216b through its regulation of CPEB4 expression influences the IL-10 level and the M2 polarization of macrophages.

qRT-PCR and ELISA analysis showed that the mRNA and the levels of IL-10 were reduced following the upregulation of miR-216b in MC38-, HCT116- and Raw264.7 cells ($P < 0.01$, **Figure 4C**, **4D**). The expressions of Ym-1, Fizz-1, Arg-1 and CD206 in Raw264.7 cells increased following treatment with MC38 CM or HCT116 CM. These effects were enhanced by CPEB4 overexpression or reversed by CPEB4 silencing ($P < 0.05$, **Figure 4E**, **4F**).

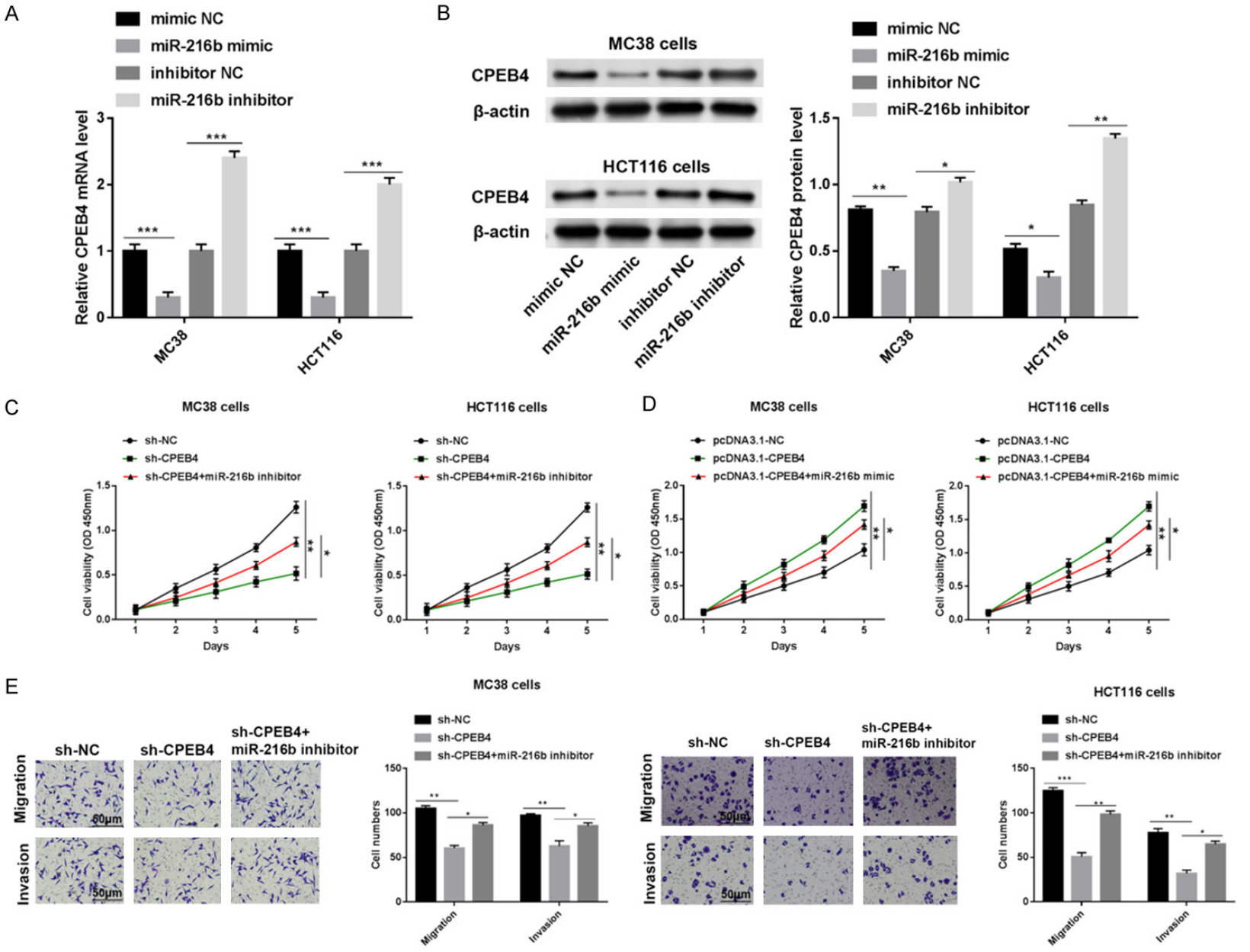
A
mimic NC
miR-216b mimic
inhibitor NC
miR-216b inhibitor
Relative CPEB4 mRNA level
MC38
HCT116
B
MC38 cells
CPEB4
β-actin
HCT116 cells
mimic NC
miR-216b mimic
inhibitor NC
miR-216b inhibitor
Relative CPEB4 protein level
C
MC38 cells
HCT116 cells
sh-NC
sh-CPEB4
sh-CPEB4+miR-216b inhibitor
Cell viability (OD 450nm)
Days
D
pcDNA3.1-NC
pcDNA3.1-CPEB4
pcDNA3.1-CPEB4+miR-216b mimic
E
sh-NC
sh-CPEB4
sh-CPEB4+ miR-216b inhibitor
Migration
Invasion
50μm
Cell numbers

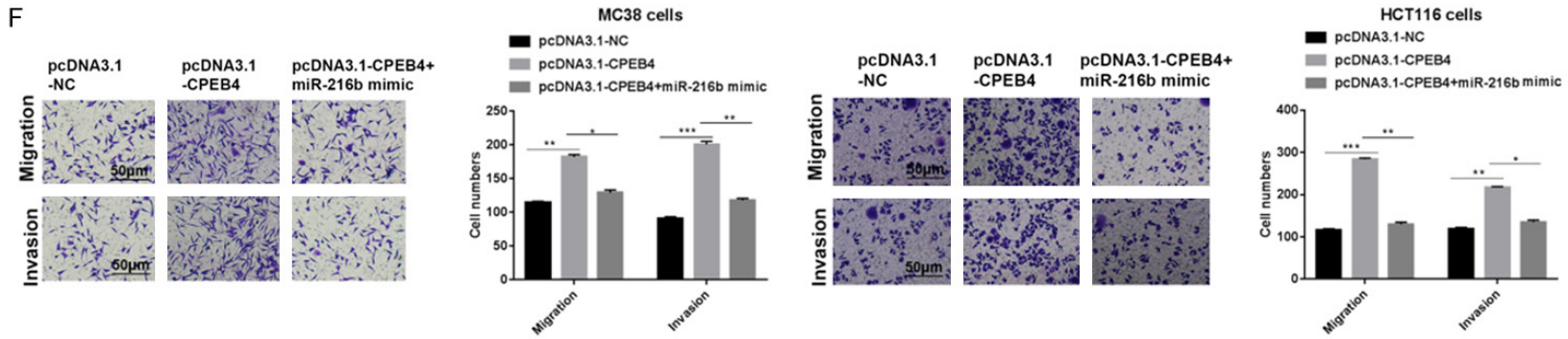

Figure 3. miR-216b suppresses the progression of colorectal cancer through targeting CPEB4. A. Relative mRNA expressions of CPEB4 in MC38 and HCT116 cells examined by qRT-PCR. B. Relative expressions of CPEB4 in MC38 and HCT116 cells assessed by Western blotting. C, D. Proliferation of MC38 and HCT116 cells assessed by cell counting kit-8 assays. E, F. Number of migrating and invading MC38 and HCT116 cells assessed by Transwell assays. $^{*}P < 0.05$, $^{**}P < 0.01$, $^{***}P < 0.001$.

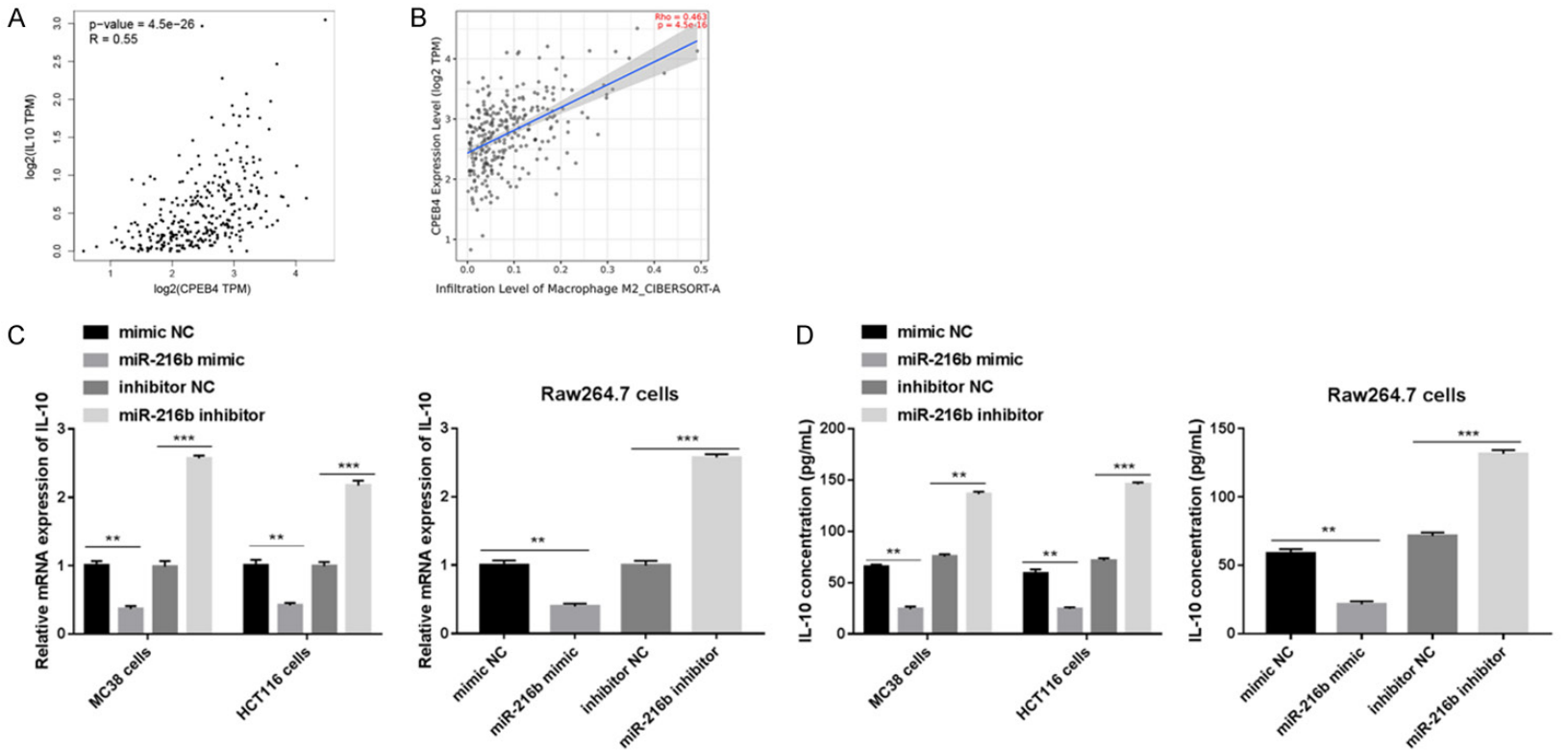

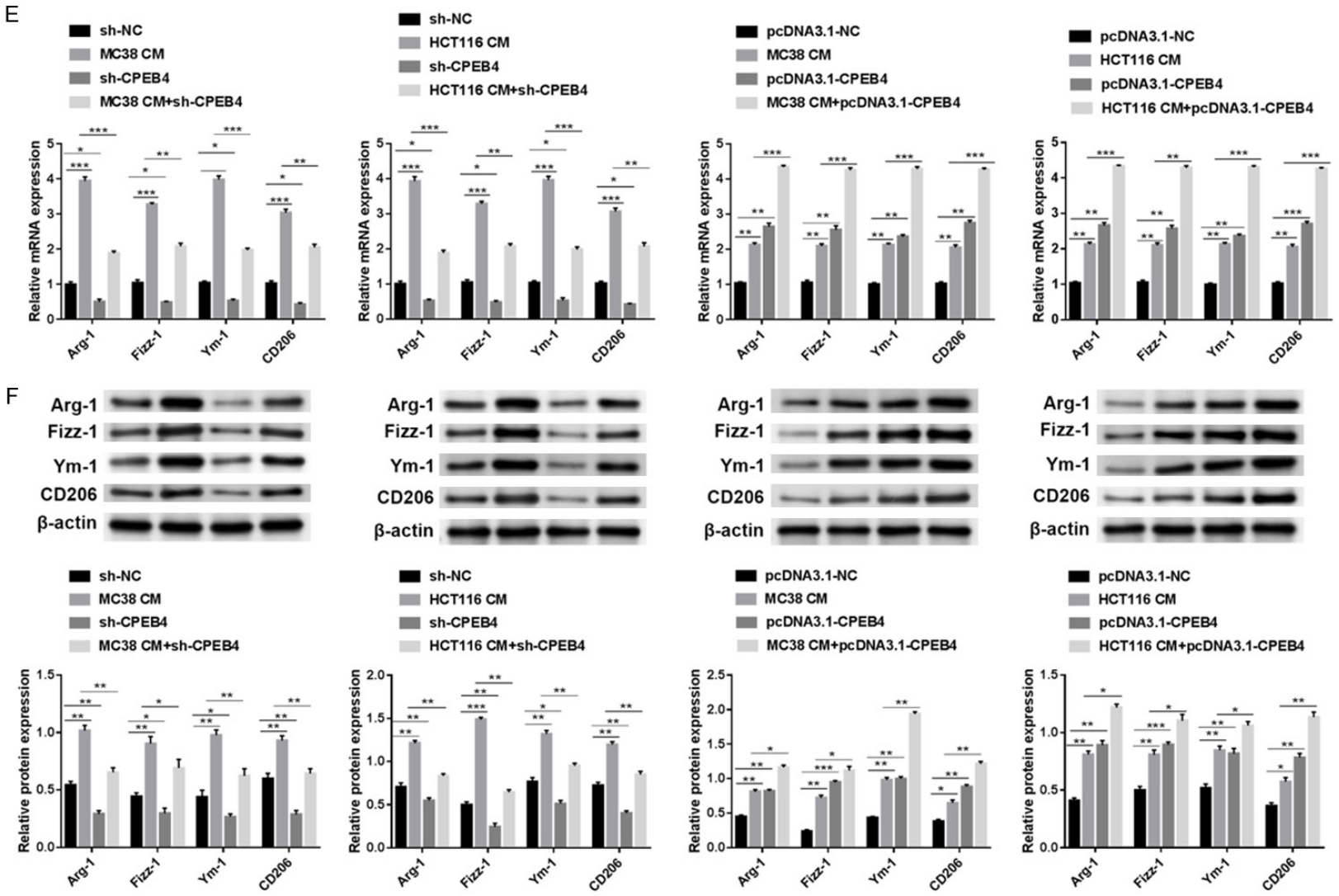

Figure 4. miR-216b impairs IL-10 expression and the M2 polarization of macrophages by regulating CPEB4 expression. (A, B) Correlation analysis between CPEB4 expression and the infiltration of M2 macrophages or between IL-10 and CPEB4 expressions. (C) mRNA levels of IL-10 determined by qRT-PCR. (D) Levels of IL-10 determined by ELISA. (E) Relative mRNA and (F) protein expressions of Arg-1, Fizz-1, Ym-1 and CD206 in Raw264.7 cells detected by qRT-PCR and Western blotting, respectively. $^{*}P < 0.05$, $^{**}P < 0.01$, $^{***}P < 0.001$.

MiR-216b impairs the IL-10-mediated M2 polarization of macrophages through its suppression of CPEB4 in CRC

CPEB4 silencing reduced the viability, migration and invasiveness of Raw264.7 cells, which increased following CPEB4 overexpression ($P < 0.05$, **Figure 5A-D**). MC38 CM or HCT116 CM also increased Raw264.7 cell viability, migration and invasiveness, which were reversed by CPEB4 knockdown ($P < 0.05$, **Figure 5A-D**) or further enhanced following CPEB4 overexpression ($P < 0.05$, **Figure 5A-D**).

The percentage of F4/80+/CD206+RAW264.7 cells (M2 macrophages) decreased following the downregulation of CPEB4, but increased following CPEB4 overexpression ($P < 0.05$, **Figure 5E**, **5F**). The abilities of MC38 CM or HCT116 CM to increase the percentage of F4/80+/CD206+RAW264.7 cells were also reversed by CPEB4 knockdown ($P < 0.05$, **Figure 5E**, **5F**) but enhanced by CPEB4 overexpression ($P < 0.05$, **Figure 5E**, **5F**).

The expression of IL-10 was reduced following CPEB4 knockdown and increased following CPEB4 overexpression ($P < 0.05$, **Figure 5G**, **5H**). The ability of MC38 CM or HCT116 CM to increase IL-10 level was reversed by CPEB4 knockdown ($P < 0.05$, **Figure 5G**, **5H**) but enhanced by its overexpression ($P < 0.05$, **Figure 5G**, **5H**).

MiR-216b interacts with CPEB4 to facilitate CRC progression via IL-10-mediated M2 polarization of TAMs in vivo

To further confirm the influence of miR-216b on tumor growth and TAMs polarization *in vivo*, a xenograft mouse model of CRC was constructed. miR-216b overexpression suppressed tumor growth in mice, leading to lower tumor volumes and weights ($P < 0.05$, **Figure 6A**). The levels of IL-10 in the serum of mice also decreased following miR-216b overexpression ($P < 0.001$, **Figure 6B**). In tumor tissues, miR-216b overexpression also reduced the expressions of CPEB4 and IL-10 ($P < 0.001$, **Figure 6C**). IHC staining similarly revealed a loss of CPEB4, CD206 and IL-10 expressions in the tumor tissue following miR-216b overexpression ($P < 0.05$, **Figure 6D**). To evaluate influences of miR-216b on liver and lung metastasis of tumor cells, we collected liver and lung tissues to perform H&E staining. It was found that liver and lung metastasis of tumor cells was evidently alleviated in response to miR-216b overexpression ($P < 0.01$, **Figure 6E**).

Discussion

A wealth of evidence has highlighted how TAMs in the TME polarize into M2-like macrophages, which facilitates the metastasis of tumor cells in CRC [13, 14, 34]. In this study, conditioned medium from CRC cells was used to simulate the TME based on previous studies [35, 36]. We observed that conditioned medium from CRC cells enhances the M2 polarization of Raw264.7 cells, which was accompanied by increased expression of M2 surface markers in M2 macrophages (Arg-1, Fizz-1, Ym-1 and CD206). In previous studies, miR-216b was shown to suppress CRC development [23-25]. Here, we showed that the upregulation of miR-216b suppressed the M2 polarization of RAW264.7 cells *in vitro*. These findings implicate miR-216b as a modulator of the TME through macrophage polarization. *In vivo* experiments confirmed these findings, since the upregulation of miR-216b suppressed CRC tumor growth and the M2 polarization of tumor cells in mice. miR-216b overexpression also decreased both the lung and liver metastasis of tumor cells in mice. Together, these data revealed new mechanistic insight into the antitumor effects of miR-216b, and highlighted its delivery to tumor cells as a promising strategy for CRC therapy.

It is well documented that CPEB4 is highly expressed in CRC tissues [29, 37] and that its downregulation suppresses the proliferation of CRC cells [38]. In our functional analysis, we confirmed that CPEB4 knockdown reduces CRC cell proliferation, migration and invasion [38]. CPEB4 also increases the expression of lncRNA RP11-361F15.2, and facilitates the development of osteosarcoma and the M2-like polarization of TAMs through the upregulation of CPEB4 *in vitro* [28]. Similarly, we discovered that CPEB4 contributed to the M2-like polarization of Raw264.7 cells. CPEB4 is a downstream target of several miRNAs in multiple cancers, including miR-758-3p in cervical cancer, miR-145-5p in glioma and miR-874-3p in endometrial cancer [30-32]. We therefore predicted that CPEB4 is targeted by miR-216b. We found

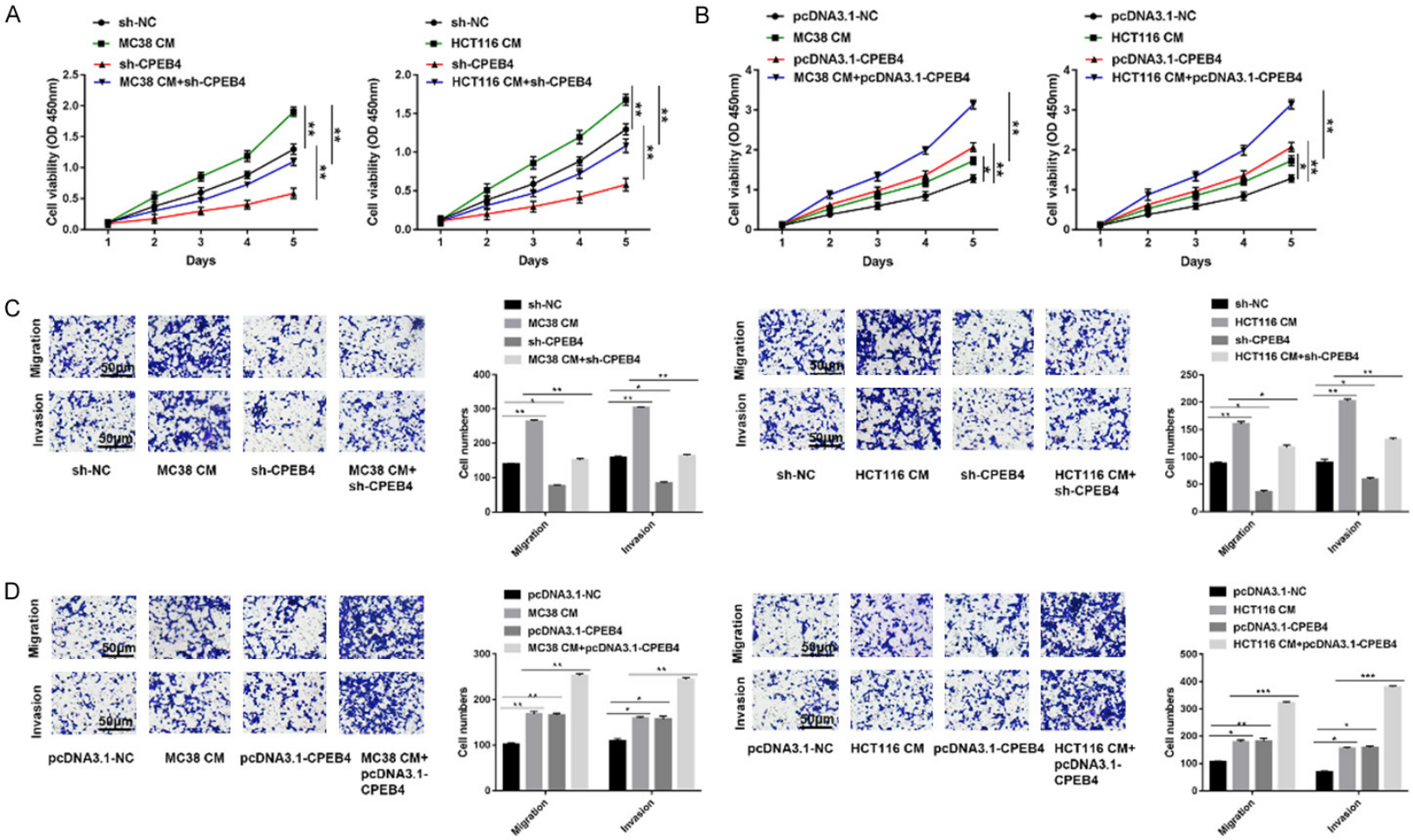
A
sh-NC
MC38 CM
sh-CPEB4
MC38 CM+sh-CPEB4
Cell viability (OD 450nm)
Days
sh-NC
HCT116 CM
sh-CPEB4
HCT116 CM+sh-CPEB4
B
pcDNA3.1-NC
MC38 CM
pcDNA3.1-CPEB4
MC38 CM+pcDNA3.1-CPEB4
pcDNA3.1-NC
HCT116 CM
pcDNA3.1-CPEB4
HCT116 CM+pcDNA3.1-CPEB4
C
Migration
Invasion
50μm
sh-NC
MC38 CM
sh-CPEB4
MC38 CM+ sh-CPEB4
Cell numbers
HCT116 CM
HCT116 CM+ sh-CPEB4
D
pcDNA3.1-NC
MC38 CM+pcDNA3.1-CPEB4
MC38 CM+ pcDNA3.1-CPEB4
HCT116 CM+pcDNA3.1-CPEB4
HCT116 CM+ pcDNA3.1-CPEB4

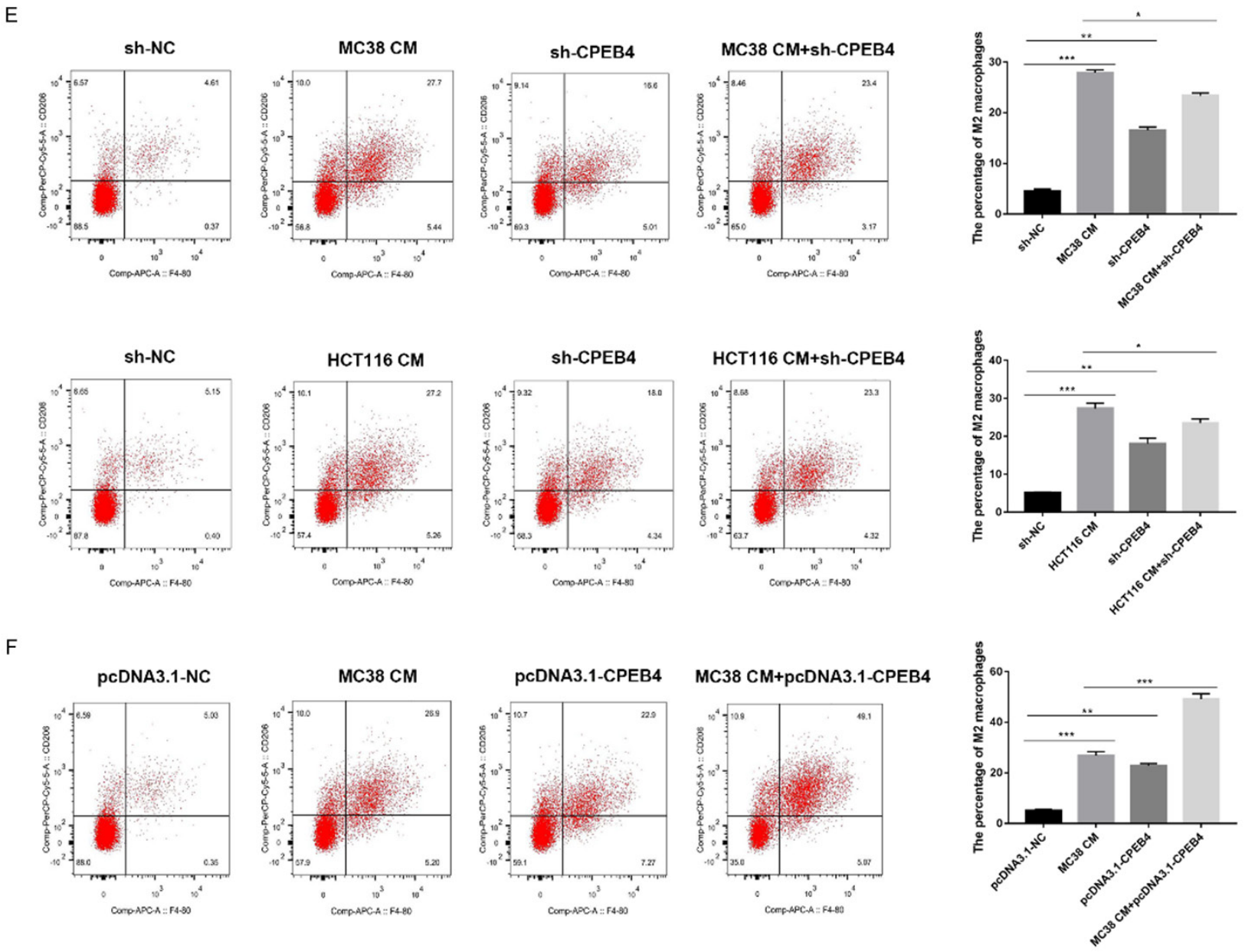
E
sh-NC
MC38 CM
sh-CPEB4
MC38 CM+sh-CPEB4
6.57
4.61
88.5
0.37
10.0
27.7
56.8
5.44
9.14
16.6
69.3
5.01
8.46
23.4
65.0
3.17
Comp-PerCP-Cy5-5-A :: CD206
Comp-APC-A :: F4-80
The percentage of M2 macrophages
sh-NC
MC38 CM
sh-CPEB4
MC38 CM+sh-CPEB4
sh-NC
HCT116 CM
sh-CPEB4
HCT116 CM+sh-CPEB4
6.66
5.15
87.8
0.40
10.1
27.2
57.4
5.26
9.32
18.0
68.3
4.34
8.68
23.3
63.7
4.32
HCT116 CM
HCT116 CM+sh-CPEB4
F
pcDNA3.1-NC
MC38 CM
pcDNA3.1-CPEB4
MC38 CM+pcDNA3.1-CPEB4
6.59
5.03
88.0
0.36
10.0
26.9
57.9
5.20
10.7
22.9
59.1
7.27
10.9
49.1
35.0
5.07
pcDNA3.1-NC
MC38 CM
pcDNA3.1-CPEB4
MC38 CM+pcDNA3.1-CPEB4

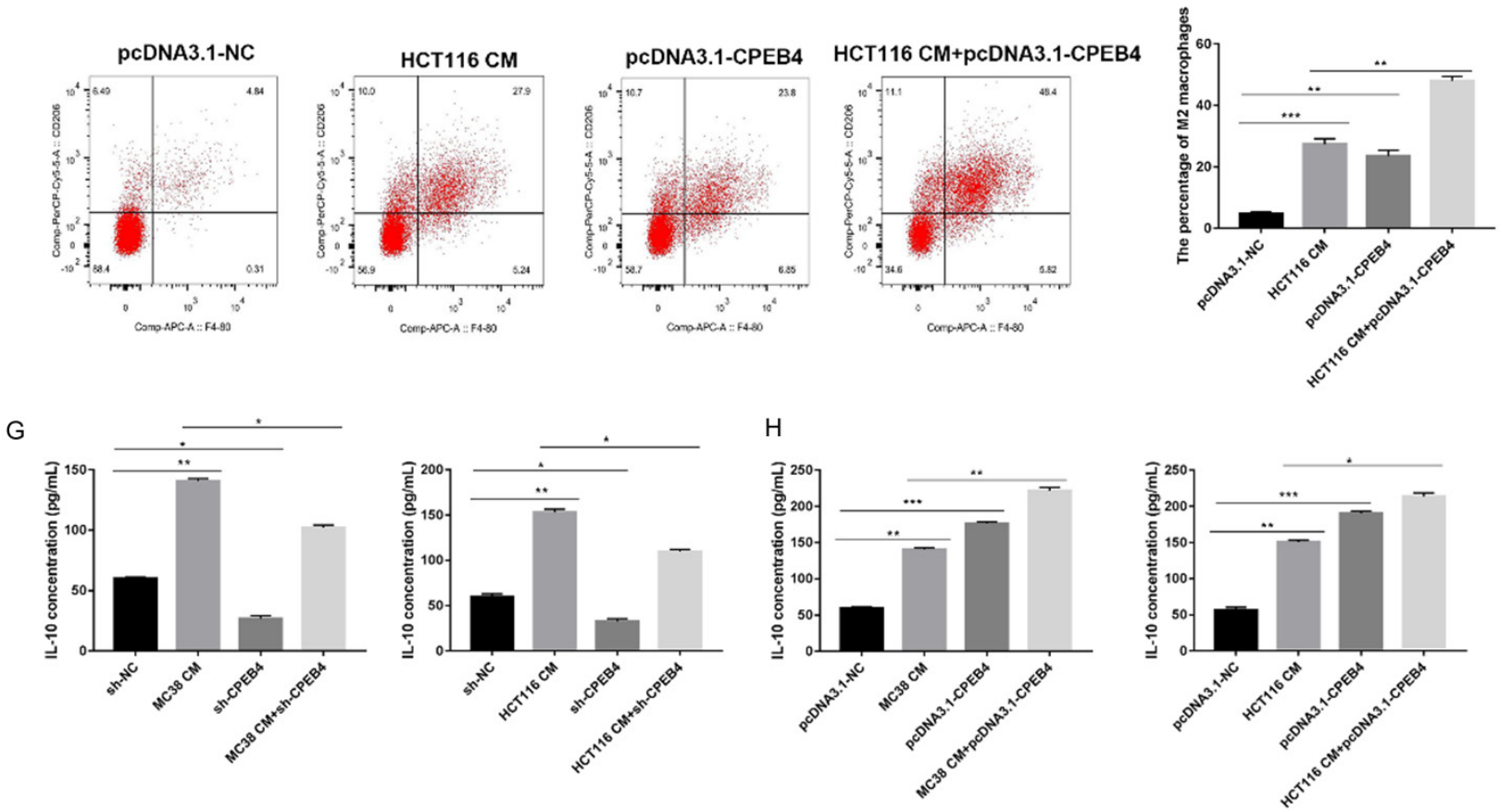

Figure 5. miR-216b impairs the IL-10-mediated M2 polarization of macrophages via a reduction in CPEB4 expression in colorectal cancer. A, B. Proliferation of Raw264.7 cells assessed by cell counting kit-8 assay. C, D. Number of migrating and invading Raw264.7 cells assessed by Transwell assays. E, F. Flow cytometry assessment of the percentage of F4/80+/CD206+RAW264.7 cells. G, H. Levels of IL-10 in Raw264.7 cells determined by ELISA. $^{*}P < 0.05$, $^{**}P < 0.01$, $^{***}P < 0.001$.

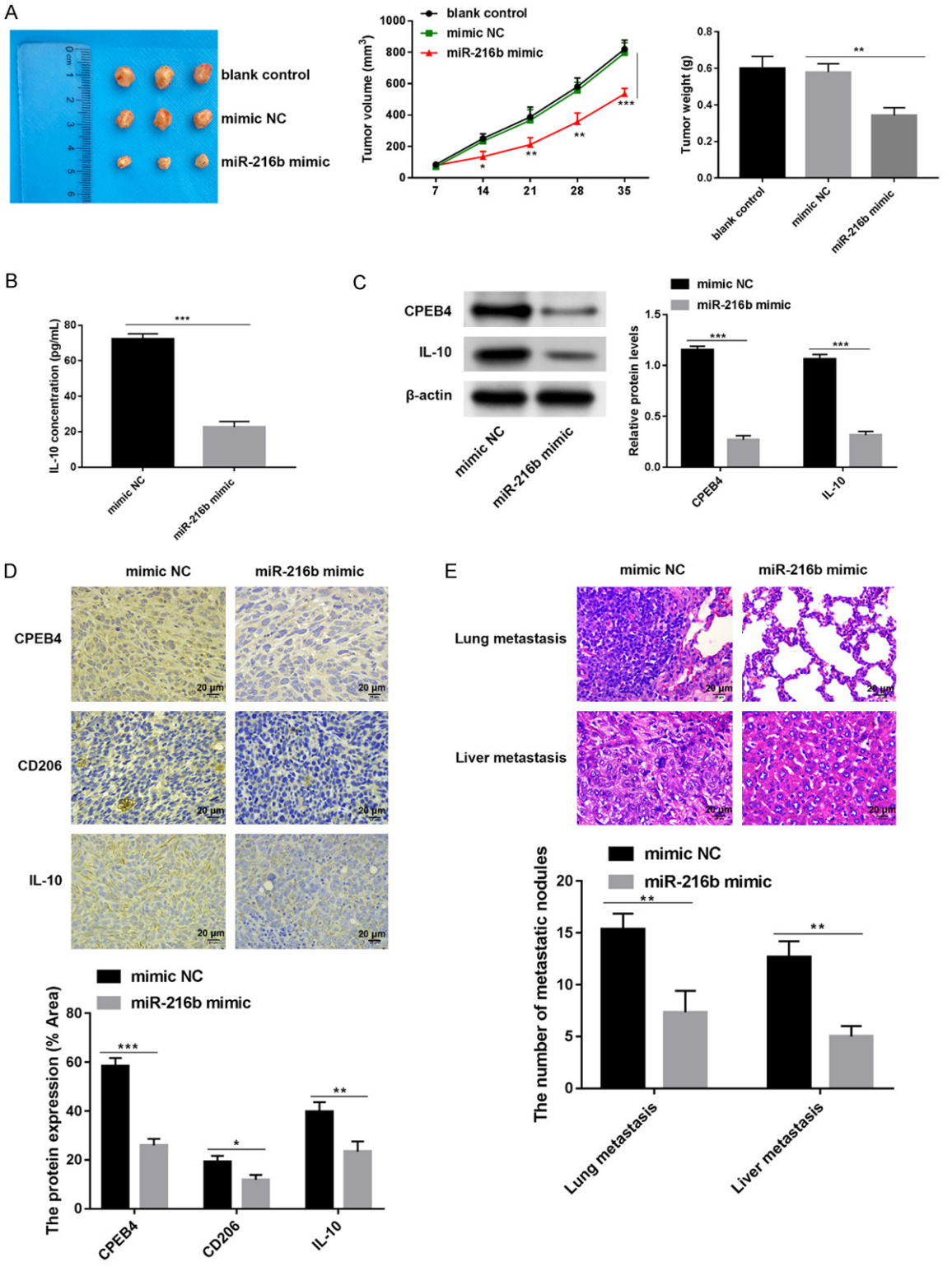

Figure 6. miR-216b interacts with CPEB4 to facilitate colorectal cancer progression via the IL-10-mediated M2 polarization of tumor-associated macrophages *in vivo*. A. Representative images of tumor in xenotransplantation mice and xenotransplantation mice transfected with miRNA mimic; compared with NC mimic group, $^{*}P < 0.05$, $^{**}P < 0.01$, $^{***}P < 0.001$. B. Levels of IL-10 in the serum of mice measured by ELISA; $^{***}P < 0.001$. C. Relative protein expressions of CPEB4 and IL-10 in tumor tissues assessed by Western blot; $^{***}P < 0.001$. D. Protein expressions of CPEB4, CD206 and IL-10 in tumor tissues determined by immunohistochemical staining and quantified by Image J software; $^{*}P < 0.05$, $^{**}P < 0.01$, $^{***}P < 0.001$. E. H&E staining to evaluate the metastasis of tumor cells in the liver and lung tissues of mice; $^{**}P < 0.01$.

that the downregulation of miR-216b abolished the suppressive influence of CPEB4 knockdown on the proliferation, migration and invasiveness of CRC cells. From these data, we conclude that miR-216b inhibits CRC development through the binding to- and suppression of CPEB4.

In previous studies, the M2 polarization of macrophages was found to be driven by IL-10 in cancer, including CRC [33, 39, 40]. In this study, we found that CPEB4 positively correlated with the infiltration of M2 macrophages and IL-10 in CRC, suggesting a positive correlation between IL-10 and the M2 polarization of macrophages. We therefore speculated that miR-216b targets CPEB4 to promote the IL-10-mediated M2 polarization of macrophages, and provided several lines of evidence to support this. We found that the levels of IL-10 decreased in response to addition of an miR-216b mimic in CRC cells and Raw264.7 cells. Also, the effects of CRC cell-derived conditioned medium on the M2 polarization of Raw264.7 cells could be reversed by CPEB4 knockdown. Furthermore, the impact of CRC cell-derived conditioned medium on the migration, invasion and proliferation of Raw264.7 cells were reversed by CPEB4 knockdown. The impact of CRC cell-derived conditioned medium on IL-10 levels were similarly reversed by CPEB4 silencing in Raw264.7 cells. These observations provide new insight into the mechanisms of CRC inhibition through the suppression of M2 polarization.

Some limitations in this study should be discussed. Firstly, we failed to validate the effects of the miR-216b/CPEB4 axis on the M2 polarization of macrophages in response to IL-10. Secondly, further *in vivo* models of CRC are required to support the findings of our *in vitro* experiments.

Conclusion

In summary, we found that miR-216b could suppress the M2 polarization of macrophages *in vitro* and *in vivo*. Mechanistically, miR-216b directly interacted with CPEB4 to impair CRC development and the IL-10-mediated M2 polarization of macrophages. These findings shed new light on the role of the miR-216b/CPEB4 axis in the M2-like polarization of macrophages and provide a mechanistic basis for the M2 macrophage-induced development of CRC.

Disclosure of conflict of interest

None.

Address correspondence to: Jiangtao Li, Department of Hepato-Biliary-Pancreatic Surgery, The First Affiliated Hospital, Hengyang Medical School, University of South China, No. 69, Chuanshan Road, Hengyang 421001, Hunan, China. Tel: +86-15073465997; E-mail: lijiangtao5997@163.com

References

[1] Baidoun F, Elshiwy K, Elkeraie Y, Merjaneh Z, Khoudari G, Sarmini MT, Gad M, Al-Husseini M and Saad A. Colorectal cancer epidemiology: recent trends and impact on outcomes. Curr Drug Targets 2021; 22: 998-1009.

[2] Sung H, Ferlay J, Siegel RL, Laversanne M, Soerjomataram I, Jemal A and Bray F. Global cancer statistics 2020: GLOBOCAN estimates of incidence and mortality worldwide for 36 cancers in 185 countries. CA Cancer J Clin 2021; 71: 209-249.

[3] Cheng L, Eng C, Nieman LZ, Kapadia AS and Du XL. Trends in colorectal cancer incidence by anatomic site and disease stage in the United States from 1976 to 2005. Am J Clin Oncol 2011; 34: 573-580.

[4] Barrios CH, Reinert T and Werutsky G. Global breast cancer research: moving forward. Am Soc Clin Oncol Educ Book 2018; 38: 441-450.

[5] Nabors LB, Portnow J, Ahluwalia M, Baehring J, Brem H, Brem S, Butowski N, Campian JL, Clark SW, Fabiano AJ, Forsyth P, Hattangadi-Gluth J, Holdhoff M, Horbinski C, Junck L, Kaley T, Kumthekar P, Loeffler JS, Mrugala MM, Nagpal S, Pandey M, Parney I, Peters K, Puduvalli VK, Robins I, Rockhill J, Rusthoven C, Shonka N, Shrieve DC, Swinnen LJ, Weiss S, Wen PY, Willmarth NE, Bergman MA and Darlow SD. Central nervous system cancers, version 3.2020, NCCN clinical practice guidelines in oncology. J Natl Compr Canc Netw 2020; 18: 1537-1570.

[6] Al Bandar MH and Kim NK. Current status and future perspectives on treatment of liver metastasis in colorectal cancer (Review). Oncol Rep 2017; 37: 2553-2564.

[7] Siegel RL, Miller KD, Fedewa SA, Ahnen DJ, Meester RGS, Barzi A and Jemal A. Colorectal cancer statistics, 2017. CA Cancer J Clin 2017; 67: 177-193.

[8] Maman S and Witz IP. A history of exploring cancer in context. Nat Rev Cancer 2018; 18: 359-376.

[9] Quail DF and Joyce JA. Microenvironmental regulation of tumor progression and metastasis. Nat Med 2013; 19: 1423-1437.

[10] Lopez-Soto A, Gonzalez S, Smyth MJ and Galluzzi L. Control of metastasis by NK cells. Cancer Cell 2017; 32: 135-154.
[11] Crespo J, Sun H, Welling TH, Tian Z and Zou W. T cell anergy, exhaustion, senescence, and stemness in the tumor microenvironment. Curr Opin Immunol 2013; 25: 214-221.
[12] Noy R and Pollard JW. Tumor-associated macrophages: from mechanisms to therapy. Immunity 2014; 41: 49-61.
[13] Wei C, Yang C, Wang S, Shi D, Zhang C, Lin X, Liu Q, Dou R and Xiong B. Crosstalk between cancer cells and tumor associated macrophages is required for mesenchymal circulating tumor cell-mediated colorectal cancer metastasis. Mol Cancer 2019; 18: 64.
[14] Lin X, Wang S, Sun M, Zhang C, Wei C, Yang C, Dou R, Liu Q and Xiong B. miR-195-5p/NOTCH2-mediated EMT modulates IL-4 secretion in colorectal cancer to affect M2-like TAM polarization. J Hematol Oncol 2019; 12: 20.
[15] Mantovani A, Sozzani S, Locati M, Allavena P and Sica A. Macrophage polarization: tumor-associated macrophages as a paradigm for polarized M2 mononuclear phagocytes. Trends Immunol 2002; 23: 549-555.
[16] Lu TX and Rothenberg ME. MicroRNA. J Allergy Clin Immunol 2018; 141: 1202-1207.
[17] Ebert MS and Sharp PA. Roles for microRNAs in conferring robustness to biological processes. Cell 2012; 149: 515-524.
[18] Hill M and Tran N. miRNA interplay: mechanisms and consequences in cancer. Dis Model Mech 2021; 14: dmm047662.
[19] Shinohara H, Kuranaga Y, Kumazaki M, Sugito N, Yoshikawa Y, Takai T, Taniguchi K, Ito Y and Akao Y. Regulated polarization of tumor-associated macrophages by mir-145 via colorectal cancer-derived extracellular vesicles. J Immunol 2017; 199: 1505-1515.
[20] Zhao S, Mi Y, Guan B, Zheng B, Wei P, Gu Y, Zhang Z, Cai S, Xu Y, Li X, He X, Zhong X, Li G, Chen Z and Li D. Tumor-derived exosomal miR-934 induces macrophage M2 polarization to promote liver metastasis of colorectal cancer. J Hematol Oncol 2020; 13: 156.
[21] Yang C, Dou R, Wei C, Liu K, Shi D, Zhang C, Liu Q, Wang S and Xiong B. Tumor-derived exosomal microRNA-106b-5p activates EMT-cancer cell and M2-subtype TAM interaction to facilitate CRC metastasis. Mol Ther 2021; 29: 2088-2107.
[22] Takano Y, Masuda T, Iinuma H, Yamaguchi R, Sato K, Tobo T, Hirata H, Kuroda Y, Nambara S, Hayashi N, Iguchi T, Ito S, Eguchi H, Ochiya T, Yanaga K, Miyano S and Mimori K. Circulating exosomal microRNA-203 is associated with metastasis possibly via inducing tumor-associated macrophages in colorectal cancer. Oncotarget 2017; 8: 78598-78613.
[23] Chen X, Liu X, He B, Pan Y, Sun H, Xu T, Hu X and Wang S. MiR-216b functions as a tumor suppressor by targeting HMGB1-mediated JAK2/STAT3 signaling way in colorectal cancer. Am J Cancer Res 2017; 7: 2051-2069.
[24] Yao Y, Li Q and Wang H. MiR-216b suppresses colorectal cancer proliferation, migration, and invasion by targeting SRPK1. Onco Targets Ther 2018; 11: 1671-1681.
[25] Zou J, Kuang W, Hu J and Rao H. miR-216b promotes cell growth and enhances chemosensitivity of colorectal cancer by suppressing PDZ-binding kinase. Biochem Biophys Res Commun 2017; 488: 247-252.
[26] Harvey RF, Smith TS, Mulroney T, Queiroz RML, Pizzinga M, Dezi V, Villenueva E, Ramakrishna M, Lilley KS and Willis AE. Trans-acting translational regulatory RNA binding proteins. Wiley Interdiscip Rev RNA 2018; 9: e1465.
[27] D'Ambrogio A, Nagaoka K and Richter JD. Translational control of cell growth and malignancy by the CPEBs. Nat Rev Cancer 2013; 13: 283-290.
[28] Yang D, Liu K, Fan L, Liang W, Xu T, Jiang W, Lu H, Jiang J, Wang C, Li G and Zhang X. LncRNA RP11-361F15.2 promotes osteosarcoma tumorigenesis by inhibiting M2-Like polarization of tumor-associated macrophages of CPEB4. Cancer Lett 2020; 473: 33-49.
[29] He X, Lin X, Cai M, Fan D, Chen X, Wang L, Wu X, Lan P and Wang J. High expression of cytoplasmic polyadenylation element-binding protein 4 correlates with poor prognosis of patients with colorectal cancer. Virchows Arch 2017; 470: 37-45.
[30] Xie H, Wang J and Wang B. Circular RNA Circ_0003221 promotes cervical cancer progression by regulating miR-758-3p/CPEB4 axis. Cancer Manag Res 2021; 13: 5337-5350.
[31] Liu Y, Li R, Wang X and Yang W. CircTTBK2 contributes to the progression of glioma through regulating miR-145-5p/CPEB4 axis. Cancer Manag Res 2020; 12: 8183-8195.
[32] Shi R, Zhang W, Zhang J, Yu Z, An L, Zhao R, Zhou X, Wang Z, Wei S and Wang H. CircESRP1 enhances metastasis and epithelial-mesenchymal transition in endometrial cancer via the miR-874-3p/CPEB4 axis. J Transl Med 2022; 20: 139.
[33] Liu Q, Yang C, Wang S, Shi D, Wei C, Song J, Lin X, Dou R, Bai J, Xiang Z, Huang S, Liu K and Xiong B. Wnt5a-induced M2 polarization of tumor-associated macrophages via IL-10 promotes colorectal cancer progression. Cell Commun Signal 2020; 18: 51.
[34] Ruffell B, Affara NI and Coussens LM. Differential macrophage programming in the tumor microenvironment. Trends Immunol 2012; 33: 119-126.

[35] Yu F, Jia X, Du F, Wang J, Wang Y, Ai W and Fan D. miR-155-deficient bone marrow promotes tumor metastasis. Mol Cancer Res 2013; 11: 923-936.
[36] Liu Y, Chen K, Wang C, Gong W, Yoshimura T, Liu M and Wang JM. Cell surface receptor FPR2 promotes antitumor host defense by limiting M2 polarization of macrophages. Cancer Res 2013; 73: 550-560.
[37] Chang YT, Huang CS, Yao CT, Su SL, Terng HJ, Chou HL, Chou YC, Chen KH, Shih YW, Lu CY, Lai CH, Jian CE, Lin CH, Chen CT, Wu YS, Lin KS, Wetter T, Chang CW and Chu CM. Gene expression profile of peripheral blood in colorectal cancer. World J Gastroenterol 2014; 20: 14463-14471.
[38] Zhong X, Xiao Y, Chen C, Wei X, Hu C, Ling X and Liu X. MicroRNA-203-mediated posttranscriptional deregulation of CPEB4 contributes to colorectal cancer progression. Biochem Biophys Res Commun 2015; 466: 206-213.
[39] Piao H, Fu L, Wang Y, Liu Y, Wang Y, Meng X, Yang D, Xiao X and Zhang J. A positive feedback loop between gastric cancer cells and tumor-associated macrophage induces malignancy progression. J Exp Clin Cancer Res 2022; 41: 174.
[40] Yi B, Dai K, Yan Z and Yin Z. Circular RNA PLCE1 promotes epithelial mesenchymal transformation, glycolysis in colorectal cancer and M2 polarization of tumor-associated macrophages. Bioengineered 2022; 13: 6243-6256.